arXiv:hep-ph/9910492v1 26 Oct 1999

Bicocca–FT–99–35
hep-ph/9910492
October 1999

An introduction to leading and next-to-leading BFKL*

Gavin P. Salam

INFN — Sezione di Milano,
Via Celoria 16, Milano 20133, Italy

Of late, the field of BFKL physics has been the subject of significant developments. The calculation of the NLL terms was recently completed, and they turned out to be very large. Techniques have been proposed to resum these corrections. These lectures provide an introduction to the BFKL equation and some of the recent developments, using DGLAP evolution as the starting point.

PACS numbers: 12.38.Cy

1. Introduction

Some twenty-five years ago Balitsky, Fadin, Kuraev and Lipatov (BFKL) set out to determine the high-energy behaviour of the scattering of hadronic objects within perturbative QCD. They found terms going as $(\alpha_s \ln s)^n$, where s is the squared centre-of-mass energy. Since $\ln s$ is large it can compensate the smallness of $\bar{\alpha}_s$ and thus it was necessary to sum this whole series of *leading logarithmic* (LL) terms. The result was that the cross section should grow as a power of the squared centre-of-mass energy s [1]. For the values of $\alpha_s \simeq 0.2$ that are typically relevant, this power comes out as being of the order of 0.5.

Over the past few years much experimental effort has been devoted towards observing this phenomenon, and the conclusion has consistently been that while the cross sections do rise, that rise is much slower than $s^{0.5}$ (see for example [2–6]).

The solution to this problem was to have been in the next-to-leading corrections to the BFKL equation, terms $\alpha_s(\alpha_s \ln s)^n$, which have been calculated over the past ten years [7]. The various contributions were put together last year [8, 9], and to the consternation of the community turned

* Presented at the Cracow School of Theoretical Physics, XXXIX Course, 1999. Work supported by E.U. QCDNET contract FMRX-CT98-0194.

out to be larger than the leading contribution, giving cross sections that were not even positive-definite [10, 11].

These lectures will illustrate the origin of some of the main features of both the leading and next-to-leading BFKL equations, using as a basis the constraints provided by the DGLAP equation, and follow on with a discussion, based on [12, 13], of how to solve the problems that arise at next-to-leading order.

After a brief definition of the problem in the next subsection, section 2 discusses the DGLAP equation as relevant for high-energy scattering, and shows how it can naturally be extended to the give the BFKL equation [1]. This is followed by an illustration of the lack of agreement of the latter with experimental data. Section 3 derives the main features of the next-to-leading corrections to BFKL and discusses some of the problems that ensue from their inclusion. Section 4 looks at how one can go beyond next-to-leading order and section 5 concludes.

1.1. The problem

Let us first define a little more carefully the problem to be addressed. We want to study collisions of two perturbative hadronic objects, figure 1, where the squared centre-of-mass energy s is much larger than the typical transverse scales Q^2, Q_0^2 of the two objects, which in turn are much larger than the QCD scale, Λ^2, in order for the problem to be perturbative. This is of phenomenological relevance for certain features of small-x deep-inelastic scattering (DIS) at HERA, high-energy $\gamma^*\gamma^*$ scattering at LEP and the NLC, and configurations at the Tevatron and LHC involving jets that are widely separated in rapidity. It is also of theoretical interest since the large parton densities that arise at high energies can lead to novel effects such as parton recombination and multiple perturbative scatterings.

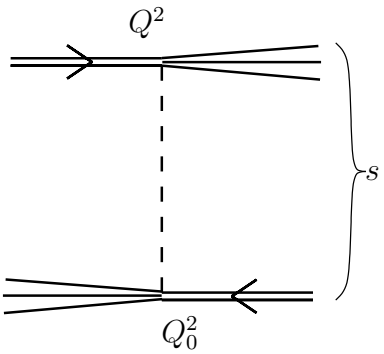

Fig. 1. High-energy collision of two hadronic objects.

2. Leading-logarithmic order

2.1. Deep inelastic scattering

Rather than entering straight into the problem of general high-energy scattering, it is helpful to consider first high-energy scattering in which one of the two hadronic objects is much smaller than the other, *i.e.* deep

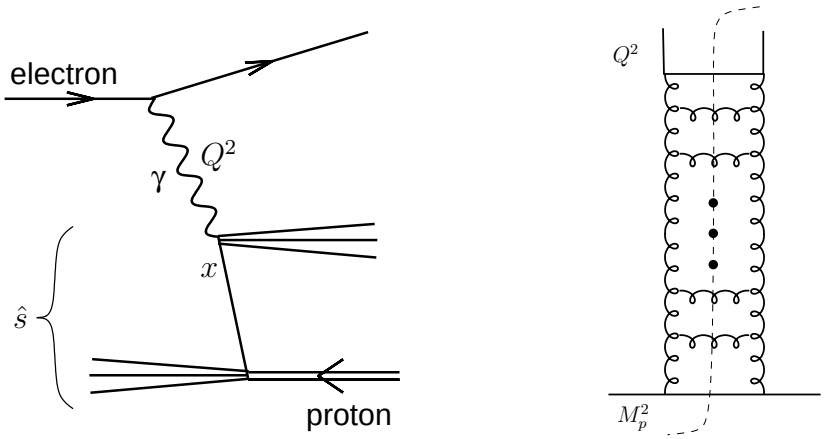

Fig. 2. (a) Deep inelastic scattering. (b) Cut ladder diagram for the evolution of the parton distributions.

inelastic scattering, figure 2a. We have the collision of a proton (of mass M_p^2, equivalent to Q_0^2 of figure 1) with a photon of virtuality $Q^2 \gg M_p^2$, which we will view as our second hadronic object. The photon-proton squared centre-of-mass energy is $\hat{s}$. High-energy scattering in this system, $\hat{s} \gg Q^2$, is generally referred to as small-x scattering because Bjorken-x is $= Q^2/\hat{s} \ll 1$.

As is well known, to correctly treat such collisions it is necessary to resum terms $(\alpha_{\rm s} \ln Q^2)^n$, because the smallness of $\alpha_{\rm s}$ is compensated by the large size of $\ln Q^2$. This is DGLAP [14] or collinear resummation, or renormalisation group evolution.

The cross section is proportional to the quark distribution at scale Q^2, which is related to the quark distribution at another scale Q_0^2 by

$$xq(x,Q^2) = xq(x,Q_0^2) + \alpha_{\rm s} \ln \frac{Q^2}{Q_0^2} \int {\rm d}z_1 \, P_{qq}(z_1) \, \frac{x}{z_1} \, q\left(\frac{x}{z_1}, Q_0^2\right) + \alpha_{\rm s} \ln \frac{Q^2}{Q_0^2} \int {\rm d}z_1 \, P_{qg}(z_1) \, \frac{x}{z_1} \, g\left(\frac{x}{z_1}, Q_0^2\right) + \ldots \quad (1)$$

In an appropriate gauge this can interpreted as the first in a set of ladder diagrams (figure 2b), whose rungs are strongly ordered in $\ln Q^2$.

To understand the type of ladder that dominates at small x, we need to look at the splitting functions. A quark ladder (with gluon rungs) involves

iteration of the P_{qq} splitting function:

$$P_{qq}(z) = \frac{C_F}{2\pi}\left[\frac{1+z^2}{(1-z)_+} + \frac{3}{2}(1-z)\right], \tag{2}$$

while a gluon ladder (with gluon rungs) involves the P_{gg} splitting function,

$$P_{gg}(z) = \frac{C_A}{\pi}\left[\frac{1}{z} + \frac{1}{(1-z)_+} - 2 + z(1-z)\right] + \delta(1-z)\beta_0\,. \tag{3}$$

At small z, P_{qq} is constant while P_{gg} grows as $1/z$. So at small x, gluon ladders with repeated iterations of $P_{gg}(z \ll 1)$ dominate, *i.e.* we have strong ordering in z.

With this is mind, let us examine the properties of the *unintegrated* gluon distribution:

$$\mathcal{F}(x,Q^2) = x\frac{\mathrm{d}g(x,Q^2)}{\mathrm{d}Q^2}\,, \tag{4}$$

and start with a simple (though not entirely physical) initial condition

$$Q^2\mathcal{F}^{(0)}(x,Q^2) = \Theta(1-x)\,\Theta\!\left(\frac{Q^2}{Q_0^2} - 1\right)\,, \tag{5}$$

where the Q^2 factor is included on dimensional grounds ($g(x,Q^2)$ is dimensionless). Using the purely gluonic DGLAP equation in differential form,

$$Q^2 x\frac{\mathrm{d}g(x,Q^2)}{\mathrm{d}Q^2} = \alpha_{\mathrm{S}}\int_x^1 \mathrm{d}z P_{gg}(z)\,\frac{x}{z}g\left(\frac{x}{z},Q^2\right), \tag{6}$$

and rewriting it in terms of the unintegrated gluon distribution, we obtain the first-order contribution to $\mathcal{F}$,

$$\begin{aligned} Q^2\mathcal{F}^{(1)}(x,Q^2) &= \alpha_{\mathrm{S}}\int_x^1 \mathrm{d}z_1 P_{gg}(z_1)\int^{Q^2}\mathrm{d}k_1^2\,\mathcal{F}^{(0)}\left(\frac{x}{z_1},k_1^2\right) \\ &\simeq \bar{\alpha}_{\mathrm{S}}\int_x^1\frac{\mathrm{d}z_1}{z_1}\int^{Q^2}\mathrm{d}k_1^2\,\mathcal{F}^{(0)}\left(\frac{x}{z_1},k_1^2\right) = \bar{\alpha}_{\mathrm{S}}\ln\frac{1}{x}\ln\frac{Q^2}{Q_0^2}\,, \end{aligned} \tag{7}$$

where $\bar{\alpha}_{\mathrm{S}} = \alpha_{\mathrm{S}}C_A/\pi$ has been introduced as a notational shorthand and a factor $\Theta(Q^2 - Q_0^2)$ is implicitly understood to be contained in the result. We retain only the $1/z$ part of the splitting function because the other parts lead to contributions lacking the factor $\ln 1/x$ and so much smaller than (7).

The second-order contribution is

$$Q^2\mathcal{F}^{(2)}(x,Q^2) = \bar{\alpha}_{\rm S}\int_x^1 \frac{{\rm d}z_2}{z_2}\int^{Q^2} {\rm d}k_2^2\,\mathcal{F}^{(1)}\left(\frac{x}{z_2},k_2^2\right) = \frac{\bar{\alpha}_{\rm S}^2}{(2!)^2}\ln^2\frac{1}{x}\ln^2\frac{Q^2}{Q_0^2}\,, \tag{8}$$

By iteration one sees that the $\mathcal{O}\left(\bar{\alpha}_{\rm S}^n\right)$ contribution is

$$Q^2\mathcal{F}^{(n)}(x,Q^2) = \frac{1}{(n!)^2}\left(\bar{\alpha}_{\rm S}\ln\frac{1}{x}\ln\frac{Q^2}{Q_0^2}\right)^n\Theta(Q^2-Q_0^2)\,. \tag{9}$$

Since every power of $\bar{\alpha}_{\rm S}$ is accompanied by two logarithms, this is referred to as a double-logarithmic (DL) series. It resums ladders in which there is strong ordering of both the transverse and longitudinal momenta along the ladders: $k_n^2/k_{n-1}^2 \gg 1$ and $z_n \ll 1$ respectively.

2.2. Summing the DL *series*

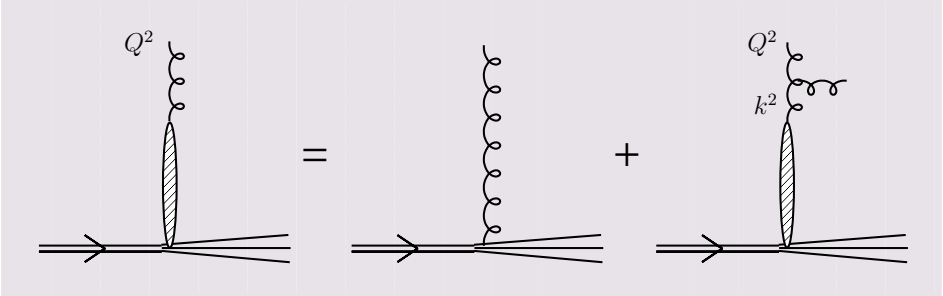

Fig. 3. Graphical depiction of the integral equation (11)

Our DL series happens to be related to the series for the modified I_0 Bessel function [15]. Using the asymptotic expansion for I_0 gives us the result that

$$Q^2\mathcal{F}(x,Q^2) \sim \exp\left[2\sqrt{\bar{\alpha}_{\rm S}\ln\frac{1}{x}\ln\frac{Q^2}{Q_0^2}}\right]\,. \tag{10}$$

However it is useful to develop a more general method of summation, one which will be applicable also later on. Accordingly, we formulate the problem as an integral equation

$$\mathcal{F}(x,Q^2) = \mathcal{F}^{(0)}(x,Q^2) + \bar{\alpha}_{\rm S}\int_x^1\frac{{\rm d}z}{z}\int^{Q^2}\frac{{\rm d}k^2}{Q^2}\mathcal{F}\left(\frac{x}{z},k^2\right), \tag{11}$$

which is depicted graphically in figure 3. It can be diagonalised by taking Mellin transforms with respect to both x and Q^2,

$$\mathcal{F}(x,Q^2) = \int \frac{\mathrm{d}\omega}{2\pi i} x^{-\omega} \int \frac{\mathrm{d}\gamma}{2\pi i} \frac{1}{Q^2} \left(\frac{Q^2}{Q_0^2}\right)^{\gamma} \mathcal{F}_{\gamma,\omega}\,, \tag{12}$$

with the contours running parallel to the imaginary axis, giving

$$\mathcal{F}_{\gamma,\omega} = \mathcal{F}^{(0)}_{\gamma,\omega} + \bar{\alpha}_{\mathrm{S}} \int_0^1 \frac{dz}{z} z^{\omega} \int^{Q^2} \frac{dk^2}{Q^2} \frac{Q^2}{k^2} \left(\frac{k^2}{Q^2}\right)^{\gamma} \mathcal{F}_{\gamma,\omega} \;=\; \mathcal{F}^{(0)}_{\gamma,\omega} + \frac{\bar{\alpha}_{\mathrm{S}}}{\omega\gamma} \mathcal{F}_{\gamma,\omega}\,. \tag{13}$$

The pole in γ is conjugate to the DGLAP logarithm of Q^2 and the pole in ω conjugate to the logarithm of x. Eq. (13) is easily solved:

$$\mathcal{F}_{\gamma,\omega} = \frac{\omega \mathcal{F}^{(0)}_{\gamma,\omega}}{\omega - \frac{\bar{\alpha}_{\mathrm{S}}}{\gamma}}\,. \tag{14}$$

With the initial condition (5), we have $\mathcal{F}^{(0)}_{\gamma,\omega} = 1/\omega\gamma$. The inverse Mellin transform with respect to ω is carried out by closing the ω contour to the left in eq. (12), leaving us with

$$Q^2\mathcal{F}(x,Q^2) = \int \frac{\mathrm{d}\gamma}{2\pi i}\, x^{-\frac{\bar{\alpha}_{\mathrm{S}}}{\gamma}} \left(\frac{Q^2}{Q_0^2}\right)^{\gamma} \cdot \frac{1}{\gamma}\,. \tag{15}$$

The integrand has a saddle-point at

$$\bar{\gamma} = \sqrt{\frac{\bar{\alpha}_{\mathrm{S}} \ln 1/x}{\ln Q^2/Q_0^2}} \tag{16}$$

and a saddle-point evaluation of the integral gives

$$Q^2\mathcal{F}(x,Q^2) \simeq \frac{1}{2} \left(\frac{1}{\pi^2 \bar{\alpha}_{\mathrm{S}} \ln\frac{1}{x} \ln\frac{Q^2}{Q_0^2}}\right)^{1/4} \exp\left[2\sqrt{\bar{\alpha}_{\mathrm{S}} \ln\frac{1}{x} \ln\frac{Q^2}{Q_0^2}}\right]. \tag{17}$$

This result was first obtained twenty-five years ago by De Rujula *et al.* [16]. Its main feature is that the gluon distribution rises at small x, with an effective power

$$\omega_{\mathrm{eff}} \simeq \sqrt{\frac{\bar{\alpha}_{\mathrm{S}} \ln 1/x}{\ln Q^2/Q_0^2}}\,, \tag{18}$$

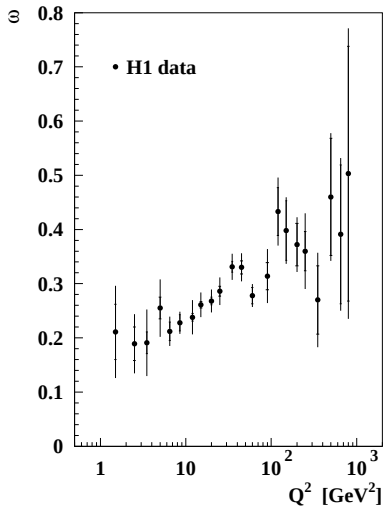

Fig. 4. The effective power of the rise of F_2 [2]; x and Q^2 values are correlated so that higher Q^2 also means higher x.

which decreases as one moves towards smaller x values, and increases towards higher Q^2. The H1 data for ω_{eff} shown in figure 4 illustrate precisely this trend. Detailed comparisons of DGLAP-induced rises of F_2, including full splitting functions and a running coupling, such as those performed by Glück, Reya and Vogt [17] and Ball and Forte [18], show remarkably good agreement with nearly all the small-x F_2 structure function data, even down to $Q^2 \simeq 4$ GeV^2.

2.3. BFKL

The above arguments are relevant in a limit where both $1/x$ and Q^2/Q_0^2 are large, *i.e.* when we have strong ordering in both longitudinal and transverse momenta. But when the ends of the chain have similar transverse momenta, $Q^2 \simeq Q_0^2$, there is no longer any reason for transverse momenta along the chain to be ordered. Double logs no longer dominate the cross section and we have to sum all leading (single) logarithms (LL) of x,

$$\left(\bar{\alpha}_{\text{S}} \ln \frac{1}{x}\right)^n. \tag{19}$$

This is done by the BFKL equation [1], which can be derived in a number of ways. Since these notes are intended only as an introduction to the BFKL

equation, rather than engaging in its derivation we will try to deduce its main characteristics from simple physical arguments.[1]

In the previous section we had the following integral equation for the gluon density (11):

$$\mathcal{F}(x,Q^2) = \mathcal{F}^{(0)}(x,Q^2) + \int \frac{\mathrm{d}z}{z} \int \mathrm{d}k^2 K(Q^2,k^2)\, \mathcal{F}\left(\frac{x}{z},k^2\right), \tag{20}$$

where the DGLAP kernel K was just

$$K(Q^2,k^2) = \frac{\bar{\alpha}_\mathrm{S}}{Q^2}\Theta(Q^2-k^2)\,, \qquad \text{valid for } Q^2 \gg k^2\,. \tag{21}$$

Since the BFKL kernel should be valid for any ratio of transverse scales it must have the same limit for $Q^2 \gg k^2$, and additionally correctly treat situations in which Q^2 is of the same order as, or much smaller than k^2. We can deduce its form in the limit $k^2 \gg Q^2$ by the following argument. The scattering of a big object off a small one, or of a small object off a big one, must have the same cross section, and both situations must be correctly described by the BFKL resummation. Therefore the BFKL kernel must be symmetric under the interchange of Q^2 and k^2. So when $k^2 \gg Q^2$ (the anti-DGLAP, or anti-collinear limit) we have

$$K(Q^2,k^2) = \frac{\bar{\alpha}_\mathrm{S}}{k^2}\,, \qquad \text{valid for } k^2 \gg Q^2\,. \tag{22}$$

If we approximate the full kernel just by its collinear and anti-collinear limits, then we have

$$K^{\mathrm{coll}}(Q^2,k^2) = \bar{\alpha}_\mathrm{S} \cdot \left(\frac{\Theta(Q^2-k^2)}{Q^2} + \frac{\Theta(k^2-Q^2)}{k^2}\right). \tag{23}$$

Following the treatment of the previous section, we will need its Mellin transform,

$$\chi^{\mathrm{coll}}(\gamma) = \frac{1}{\gamma} + \frac{1}{1-\gamma}\,, \tag{24}$$

where, by convention, the leading factor of $\bar{\alpha}_\mathrm{S}$ has been left out; $\chi(\gamma)$ is usually referred to as the *characteristic function* of the system. The $1/\gamma$ term was present also in the pure DGLAP case, and comes from the collinear limit. The $1/(1-\gamma)$ term comes from the anti-collinear limit. The symmetry

[1] For the interested reader one of the simplest full derivations is perhaps to be found within the dipole formulation [19]. A wide ranging introduction and discussion of many aspects of BFKL physics can be found in [20].

$\gamma \leftrightarrow 1-\gamma$ is a direct consequence of the symmetry under the exchange of the two transverse scales. This can be seen explicitly from the definition of the Mellin transform, eq. (12), where

$$\frac{1}{Q^2}\left(\frac{Q^2}{Q_0^2}\right)^{\gamma} = \frac{1}{Q_0^2}\left(\frac{Q_0^2}{Q^2}\right)^{1-\gamma}. \tag{25}$$

What we have neglected in our collinear + anti-collinear approximation is the correct treatment of the kernel for k of the same order as Q. This is given by the full BFKL kernel [1] (with integration measure d^2k/π because the azimuthal integration now matters):

$$K(Q^2,k^2) = \bar{\alpha}_{\mathrm{S}} \cdot \left(\frac{1}{|\vec{Q}-\vec{k}|^2} - \delta(Q^2-k^2)\int^k \frac{\mathrm{d}^2q}{\pi q^2}\right). \tag{26}$$

Its Mellin transform (again leaving out the overall factor of $\bar{\alpha}_{\mathrm{S}}$) is

$$\chi(\gamma) = 2\psi(1) - \psi(\gamma) - \psi(1-\gamma), \tag{27}$$

where $\psi(x) = \mathrm{d}\ln\Gamma(x)/\mathrm{d}x$. Noting that $-\psi(\gamma) = 1/\gamma + \mathcal{O}(1)$ for small x, we see that the full $\chi(\gamma)$ has the same polar structure around $\gamma = 0$ and $\gamma = 1$ as our approximation (24) reflecting the fact that the collinear and anti-collinear limits are the same. The two characteristic functions are shown in fig. 5, which illustrates their very similar shapes: they differ by little more than a constant.

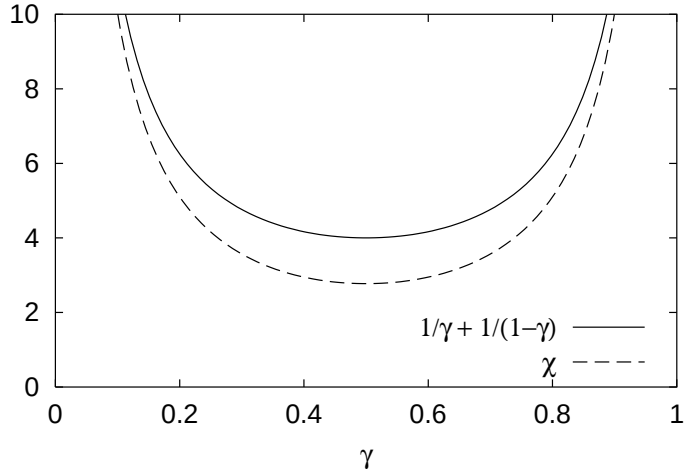

Fig. 5. The full and collinearly-approximated characteristic functions.

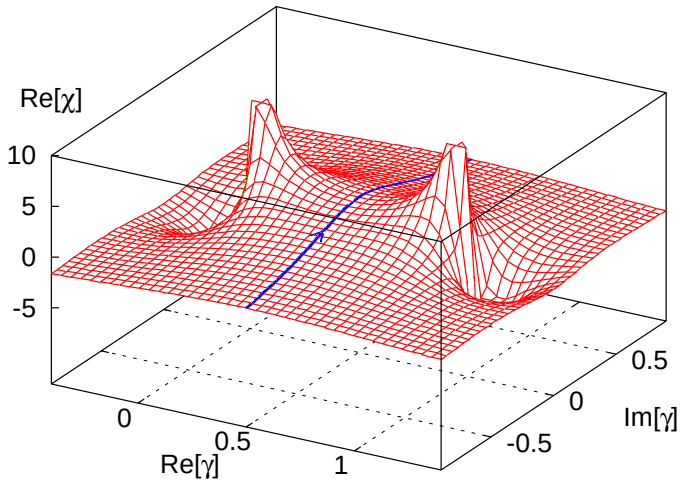

Fig. 6. The real part of the LL BFKL characteristic function in the complex plane and the integration contour for the inverse Mellin transform.

The procedure for obtaining the BFKL cross section is analogous to that used in the DGLAP case, with $1/\gamma$ replaced by $\chi(\gamma)$. We start with the Mellin-transformed integral equation

$$\mathcal{F}_{\gamma,\omega} = \mathcal{F}^{(0)}_{\gamma,\omega} + \frac{\bar{\alpha}_{\mathrm{S}}}{\omega}\chi(\gamma)\mathcal{F}_{\gamma,\omega}\,, \tag{28}$$

and solve for $\mathcal{F}_{\gamma,\omega}$:

$$\mathcal{F}_{\gamma,\omega} = \frac{\omega\mathcal{F}_{\gamma,\omega}}{\omega - \bar{\alpha}_{\mathrm{S}}\chi(\gamma)} \tag{29}$$

The inverse Mellin transform with respect to ω is once again trivial and gives

$$\mathcal{F}(x,Q^2) = \int \frac{\mathrm{d}\gamma}{2\pi i}\exp\left[\bar{\alpha}_{\mathrm{S}}\chi(\gamma)\ln\frac{1}{x} + \gamma\ln\frac{Q^2}{Q_0^2}\right]\cdot\bar{\omega}\mathcal{F}^{(0)}_{\gamma,\bar{\omega}} \qquad \bar{\omega} = \bar{\alpha}_{\mathrm{S}}\chi(\gamma)\,. \tag{30}$$

The real part of the characteristic function $\chi(\gamma)$, together with the integration contour are shown in the complex plane in figure 6. For large $\ln 1/x$, the integrand in (30) is dominated by behaviour of χ and has a saddle-point close to $\gamma = 1/2$, which causes the gluon distribution to grow as

$$\mathcal{F}(x,Q^2) \simeq \frac{x^{-\bar{\alpha}_{\mathrm{S}}\chi\left(\frac{1}{2}\right)}}{\sqrt{2\pi\,\bar{\alpha}_{\mathrm{S}}\,\chi''\left(\frac{1}{2}\right)\ln\frac{1}{x}}}\cdot\frac{1}{QQ_0}\,, \tag{31}$$

where χ'' is the second derivative of χ with respect to γ. Thus the gluon distribution (and in general, high-energy cross sections) should grow as a power of x determined by the minimum value of $\chi(\gamma)$, which is $\chi(1/2) = 4\ln 2$. For the phenomenologically reasonable value of $\bar{\alpha}_{\rm S} \simeq \alpha_{\rm S} = 0.2$ this gives a power of about 0.5.

It suffices to look back at figure 4 to see that this is incompatible with the rise seen in the bulk of the structure function data. Some care is needed in interpreting this disagreement: in considering the structure function data, we are trying to apply perturbative QCD to a problem which is inherently non-perturbative (the scale Q_0^2 does not satisfy our requirement $Q_0^2 \gg \Lambda^2$). However BFKL also predicts scaling violations of the F_2 structure function [21], and this prediction can be shown not to depend on the properties of the non-perturbative region [13, 22]. Essentially, regardless of the input distribution, the scaling violations quickly lead to a structure function which rises with a power $4\ln 2\bar{\alpha}_{\rm S}$ and so is incompatible with the data [23].

There exist other, theoretically cleaner, tests of BFKL. Generally they involve selecting a process with two hard hadronic probes, such as jets or a virtual photon, separated by a large rapidity (or equivalently having a large centre-of-mass energy). The requirement that both probes be hard ensures that one can reasonably apply perturbation theory[2] (unfortunately it generally also makes the experimental measurement much harder). A nice example of such a test is the collision of two virtual photons as measured recently by the L3 [4] and OPAL [5] collaborations. The L3 data are shown in figure 7. The data are significantly higher than the one-gluon estimate (*i.e.* the prediction without BFKL resummation). On the other hand the LL BFKL predictions clearly overshoot the data. The L3 collaboration perform a fit to the data in order to determine the power of the high-energy growth, and quote a preliminary result of 0.29 ± 0.025 for scales in the range of 3.5 to $14.5\,\mathrm{GeV}^2$ [24].[3]

The same conclusion of incompatibility with LL BFKL comes out from

[2] Though not strictly the subject of this presentation, an exposition of BFKL physics would be incomplete without at least some mention of *diffusion*. Because transverse momenta are not ordered, small-x evolution leads to a random walk in $\ln k_t$. The mean width of this random walk — diffusion — increases as $\sqrt{\ln s}$, and at very large s eventually enters into the non-perturbative region. Thus, no matter how large the transverse scales of the scattering objects, there is always an energy beyond which perturbation theory loses its predictive power.

[3] This result should probably be interpreted with some caution because the formula used to carry out the fit assumes the LL normalisation with four light-quark flavours (whereas both the NLL corrections and the charm mass probably have a significant effect on the normalisation). A fit leaving the normalisation as a free parameter leads to a similar power but with a much larger error. One should bear in mind that because of the 'limited' energies at LEP, the Q^2 values (between 3.5 and 14.5 GeV^2) are probably on the border of the region that can be considered perturbative.

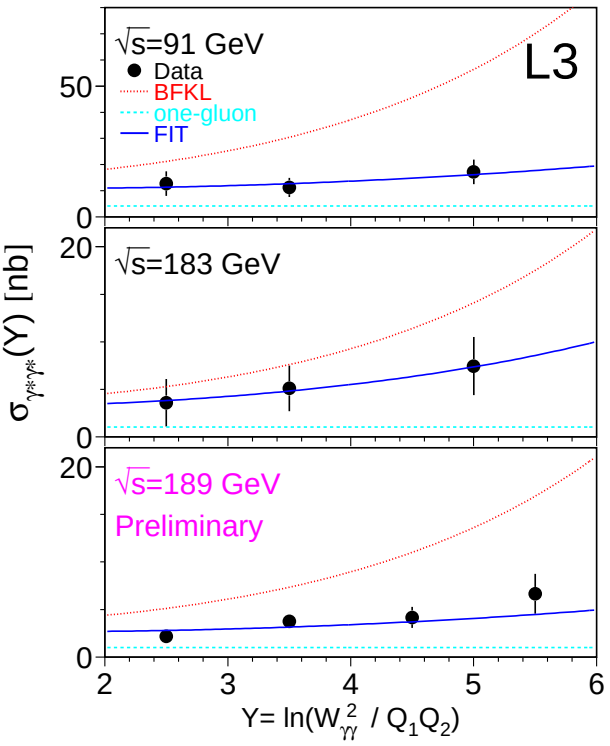

Fig. 7. The cross section for $\gamma^*\gamma^*$ collisions as measured by the L3 collaboration [4, 24]. The mean Q^2 values for the three energies are 3.5, 14 and 14.5 GeV^2 respectively.

looking at the interactions between a jet and a virtual photon in DIS [6], a measurement referred to as the forward-jet cross section, because of the position of the jet in the detector.

3. Next-to-leading corrections

All along, while the various experimental tests of LL BFKL were being carried out and refined, the calculation of the next-to-leading logarithmic corrections to BFKL was in progress. The next-to-leading terms are those suppressed by a power of α_s relative to the LL series:

$$\alpha_\mathrm{s}(\alpha_\mathrm{s}\ln s)^n\,. \tag{32}$$

In terms of the notation developed so far, this corresponds to working out the NLL corrections to the characteristic function χ, *i.e.* finding χ_1, where

$$\bar{\alpha}_{\rm s}\chi(\gamma) = \bar{\alpha}_{\rm s}\chi_0(\gamma) + \bar{\alpha}_{\rm s}^2\chi_1(\gamma) + \mathcal{O}\left(\bar{\alpha}_{\rm s}^3\right) . \tag{33}$$

The determination of χ_1 took close to ten years [7], and was completed quite recently [8, 9].

Rather than trying to reproduce parts of that derivation, we will adopt the same approach that was used in the previous section, namely to deduce the structure of the NLL corrections through a study of the collinear limit and symmetry requirements. This will translate to determining the divergences around $\gamma = 0$ and $\gamma = 1$.

We will examine three main contributions: those from the running coupling, the non-singular (at small z) part of the splitting functions and the choice of energy scale.

3.1. Running coupling

The QCD coupling runs as

$$\bar{\alpha}_{\rm s}(k^2) = \frac{\bar{\alpha}_{\rm s}(Q^2)}{1 + b\,\bar{\alpha}_{\rm s}(Q^2)\ln\frac{k^2}{Q^2}} , \tag{34}$$

where $b = 11/12 - n_f/6$. What sort of higher order contribution will this lead to? The DGLAP equations tell us that in the right-hand graph of fig. 3, when $Q^2 \gg k^2$ the correct scale for the coupling is Q^2. By symmetry, when $k^2 \gg Q^2$, the correct scale is k^2 — *i.e.* in the collinear limit the correct scale is the larger of the two scales involved. So our collinear approximation for the kernel, eq. (23), becomes

$$K^{\rm coll}(Q^2, k^2) = \bar{\alpha}_{\rm s}(Q^2)\frac{\Theta(Q^2-k^2)}{Q^2} + \bar{\alpha}_{\rm s}(k^2)\frac{\Theta(k^2-Q^2)}{k^2} . \tag{35}$$

The Mellin transform of the first term just gives $\bar{\alpha}_{\rm s}(Q^2)/\gamma$, as before. For the second term, we re-express $\bar{\alpha}_{\rm s}(k^2)$ in terms of $\bar{\alpha}_{\rm s}(Q^2)$ in order to extract a factor of $\bar{\alpha}_{\rm s}(Q^2)$ in front of the whole result. Expanding to second order, and taking the Mellin transform, gives

$$\int_{Q^2}\frac{{\rm d}k^2}{k^2}\left(\bar{\alpha}_{\rm s}(Q^2) - b\bar{\alpha}_{\rm s}^2\ln\frac{k^2}{Q^2}\right)\frac{Q^2}{k^2}\left(\frac{k^2}{Q^2}\right)^{\gamma} = \frac{\bar{\alpha}_{\rm s}(Q^2)}{1-\gamma} - \frac{b\bar{\alpha}_{\rm s}^2}{(1-\gamma)^2} , \tag{36}$$

which is just the anti-collinear part of our LL result plus a running-coupling NLL contribution

$$\chi_1^b = -\frac{b}{(1-\gamma)^2} . \tag{37}$$

The lack of symmetry $\gamma \leftrightarrow 1-\gamma$ is due to our choice to extract an asymmetric factor of $\bar{\alpha}_{\rm s}(Q^2)$ in front of the answer.

What is the uncertainty on our collinear approximation for χ_1^b? The scheme of $\bar{\alpha}_{\rm s}$ is not defined, corresponding to an uncertainty proportional to χ_0. Nor do we a priori know the correct scale for branchings when k^2 and Q^2 are of the same order. So the overall uncertainty is a function with at most single poles at $\gamma = 0$ and $\gamma = 1$.

3.2. Splitting function

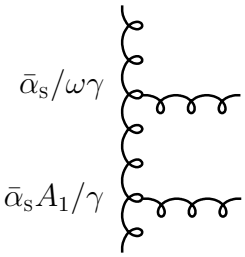

Fig. 8. A sequence of a small-x and a non-small-x branching.

In section 2 we used only the part of the gluon splitting function that is singular at small z. At NLL, we need to include the full splitting function (3). Its Mellin transform (with respect to x) is

$$P_{gg}^{\omega} = \frac{1}{\omega} + A_1(\omega)\,, \tag{38}$$

where (for $n_f = 0$)

$$A_1(\omega) = -\frac{11}{12} + \mathcal{O}\left(\omega\right)\,. \tag{39}$$

To get the NLL correction we consider a sequence of two collinear branchings, fig. 8, where one of the branchings is a small-x branching, giving a factor $\bar{\alpha}_{\rm s}/\omega\gamma$ and the other is a non-small-x branching, giving a factor $\bar{\alpha}_{\rm s}A_1/\gamma$. Remembering that convolutions in x and k^2 space translate to products in the ω, γ Mellin transform space, our integral equation (28) receives a contribution

$$\frac{\bar{\alpha}_{\rm s}}{\omega}\frac{\bar{\alpha}_{\rm s}A_1}{\gamma^2}\mathcal{F}_{\gamma,\omega}\,. \tag{40}$$

There is a corresponding term for a pair of anti-collinear branchings, so that the splitting-function contribution to χ_1 is

$$\chi_1^{A_1}(\gamma) = \frac{A_1}{\gamma^2} + \frac{A_1}{(1-\gamma)^2}\,, \tag{41}$$

where $A_1 = A_1(0) = -11/12$. Actually this is only the n_f-independent part. For non-zero n_f there are contributions coming from the n_f-dependence of P_{gg} and from diagrams involving the convolution of P_{gq} and P_{qg}.

As in the running coupling case we have an uncertainty on this result, which can arise for example from the combination of a collinear and an

anti-collinear branching, and thus is once again at the level of a function with at most single poles at $\gamma = 0$ and $\gamma = 1$.

3.3. Energy scale terms

A more subtle source of NLL corrections comes from the so-called energy-scale terms. At leading order one resums terms

$$\left(\bar{\alpha}_{\mathrm{s}} \ln \frac{s}{s_0}\right)^n , \tag{42}$$

where s_0 can be chosen arbitrarily. Changing s_0 is equivalent to introducing a whole set of higher order terms. For a symmetric treatment (with respect to Q and Q_0), a natural choice is $s_0 = Q_0 Q$. Let us then consider what happens when $Q \gg Q_0$. As we obtained in section 2.1, the leading terms are

$$\frac{1}{(n!)^2} \left(\bar{\alpha}_{\mathrm{s}} \ln \frac{s}{Q Q_0} \ln \frac{Q^2}{Q_0^2}\right)^n . \tag{43}$$

But for DIS-like situations, $Q \gg Q_0$, we usually express our results as a function of $x = Q^2/s$ and Q^2/Q_0^2. Let us do that for the $n = 2$ term:

$$\frac{1}{4}\left(\bar{\alpha}_{\mathrm{s}} \ln \frac{s}{Q Q_0} \ln \frac{Q^2}{Q_0^2}\right)^2 = \frac{1}{4}\left(\bar{\alpha}_{\mathrm{s}} \ln \frac{1}{x} \ln \frac{Q^2}{Q_0^2}\right)^2 + \frac{1}{4}\bar{\alpha}_{\mathrm{s}}^2 \ln \frac{1}{x} \ln^3 \frac{Q^2}{Q_0^2} + \mathrm{NNLL}\,. \tag{44}$$

Of particular interest is the second term on the RHS because it has more collinear logs than powers of $\bar{\alpha}_{\mathrm{s}}$ (it contains a double collinear logarithm for a single power of $\bar{\alpha}_{\mathrm{s}}$). But we know from renormalisation group constraints that the cross section written as a function of x and Q^2/Q_0^2 contains at most as many collinear logs as powers of $\bar{\alpha}_{\mathrm{s}}$. Therefore for the result to be consistent with the renormalisation group, the next-to-leading corrections must be such as to cancel the second term on the RHS of (44), *i.e.* they must contain a term

$$-\frac{1}{4}\bar{\alpha}_{\mathrm{s}}^2 \ln s \ln^3 \frac{Q^2}{Q_0^2}\,. \tag{45}$$

In Mellin transform space this will correspond to a contribution to χ_1 which is proportional to $1/\gamma^3$. To obtain its coefficient it is not sufficient just to take the Mellin transform of (45), because not all of the correction exponentiates (*i.e.* should be incorporated into χ) — for example some of it is to be associated with the initial condition.

Instead, now that we know what kind of answer to expect, let us directly consider the problem in Mellin-transform space. We start with a result written for energy scale QQ_0 (*cf.* eqs. (12) and (29)),

$$\mathcal{F}(s,Q^2) = \int \frac{\mathrm{d}\omega}{2\pi i} \int \frac{\mathrm{d}\gamma}{2\pi i} \left(\frac{s}{QQ_0}\right)^{\omega} \frac{1}{Q^2} \left(\frac{Q^2}{Q_0^2}\right)^{\gamma} \frac{\omega \mathcal{F}^{(0)}_{\gamma,\omega}}{\omega - \bar{\alpha}_{\mathrm{s}}\chi(\gamma)}\,, \tag{46}$$

and then note that since

$$\left(\frac{s}{QQ_0}\right)^{\omega} \left(\frac{Q^2}{Q_0^2}\right)^{\gamma} = \left(\frac{s}{Q^2}\right)^{\omega} \left(\frac{Q^2}{Q_0^2}\right)^{\gamma+\frac{\omega}{2}}\,, \tag{47}$$

rewriting (46) with energy scale $s_0 = Q^2$ is just equivalent to shifting $\gamma \to \gamma - \frac{\omega}{2}$ in χ and $\mathcal{F}^{(0)}$:

$$\mathcal{F}(s,Q^2) = \int \frac{\mathrm{d}\omega}{2\pi i} \int \frac{\mathrm{d}\gamma}{2\pi i} \left(\frac{s}{Q^2}\right)^{\omega} \frac{1}{Q^2} \left(\frac{Q^2}{Q_0^2}\right)^{\gamma} \frac{\omega \mathcal{F}^{(0)}_{\gamma-\frac{\omega}{2},\omega}}{\omega - \bar{\alpha}_{\mathrm{s}}\chi(\gamma-\frac{\omega}{2})}\,. \tag{48}$$

If we now expand $\chi(\gamma - \frac{\omega}{2})$ in powers of $\bar{\alpha}_{\mathrm{s}}$, recursively using the relation $\omega = \bar{\alpha}_{\mathrm{s}}\chi$ we get

$$\chi(\gamma - \frac{\omega}{2}) = \chi(\gamma) - \frac{\bar{\alpha}_{\mathrm{s}}\chi\chi'}{2} + \mathcal{O}\left(\bar{\alpha}_{\mathrm{s}}^2\right)\,. \tag{49}$$

In the collinear limit ($\gamma \to 0$), since $\chi(\gamma)$ goes as $1/\gamma$, the $\mathcal{O}\left(\bar{\alpha}_{\mathrm{s}}\right)$ piece has the behaviour

$$-\frac{\bar{\alpha}_{\mathrm{s}}\chi\chi'}{2} \simeq \frac{\bar{\alpha}_{\mathrm{s}}}{2\gamma^3}\,. \tag{50}$$

This is the analogue of the $\ln^3 Q^2$ term seen earlier (44) and it must be subtracted from χ at scale $s_0 = QQ_0$ in order for the collinear limit with energy scale Q^2 to be free of unwanted double collinear logs. There is an analogous $1/2(1-\gamma)^3$ piece to be subtracted for the anti-collinear limit to be correct (*i.e.* free of double anti-collinear logs for energy scale $s_0 = Q_0^2$). Overall therefore we have the following NLL energy-scale corrections (for $s_0 = QQ_0$):

$$\chi_1^{s_0} = -\frac{1}{2\gamma^3} - \frac{1}{2(1-\gamma)^3}\,. \tag{51}$$

As was the case for the running coupling and splitting function terms, our analysis leaves us with an uncertainty which amounts to a function with at most single poles at $\gamma = 0$ and $\gamma = 1$.

3.4. Putting things together

Putting together eqs. (37), (41) and (51) gives us the following answer for the collinearly-enhanced part of the NLL corrections ($n_f = 0$):

$$\chi_1^{\rm coll}(\gamma) = \frac{A_1}{\gamma^2} + \frac{A_1 - b}{(1-\gamma)^2} - \frac{1}{2\gamma^3} - \frac{1}{2(1-\gamma)^3}\,, \tag{52}$$

with $A_1 = -11/12$. Our collinear approximation guarantees the correctness of the coefficients of the cubic and quadratic divergences at $\gamma = 0$ and $\gamma = 1$.

The true NLL corrections as assembled in [8, 9] are, in the $\overline{\rm MS}$ scheme and for $n_f = 0$ (the n_f dependence turns out to be small)

$$\begin{aligned}\chi_1(\gamma) = &-\frac{\pi^2\cos(\pi\gamma)}{4\sin^2(\pi\gamma)(1-2\gamma)}\left(3 + \frac{2+3\gamma(1-\gamma)}{(3-2\gamma)(1+2\gamma)}\right)\\ &-\frac{b}{2}\left(\chi_0^2(\gamma) - \psi'(\gamma) + \psi'(1-\gamma)\right) + \frac{\psi''(\gamma)}{4} + \frac{\psi''(1-\gamma)}{4}\\ &+\left(\frac{67}{36} - \frac{\pi^2}{12}\right)\chi_0(\gamma) + \frac{3}{2}\zeta(3) + \frac{\pi^3}{4\sin(\pi\gamma)} - \phi(\gamma)\,,\end{aligned} \tag{53}$$

where

$$\phi(\gamma) = \sum_{n=0}^{\infty}(-1)^n\left[\frac{\psi(n+1+\gamma) - \psi(1)}{(n+\gamma)^2} + \frac{\psi(n+2-\gamma) - \psi(1)}{(n+1-\gamma)^2}\right]. \tag{54}$$

It is possible to make a direct identification between parts of (53) and (52) in terms of the coefficients of the double and triple poles. The first line of (53) is identifiable with the A_1 piece of (52) and so originates from the splitting function. The running-coupling dependence enters through the first term on the second line of (53), while the energy-scale dependent piece is formed by the last two terms of that line. The remaining terms are free of double and triple poles. Of these terms, so far only the first one on the third line of (53) has been understood: it is associated with the fact that the natural scheme for processes involving soft gluons is the CMW or gluon-bremsstrahlung scheme [25]. When writing an answer in the $\overline{\rm MS}$ scheme this leads to a correction term which is $(67/36 - \pi^2/12)\bar{\alpha}_{\rm s}$ times the leading order result.

Figure 9 shows the full χ_1 together with our collinear approximation. There is a remarkable similarity between them: in the range $0 < \gamma < 1$ they never differ by more than 7%. Possible reasons for the surprisingly good agreement will be discussed later, in section 4.

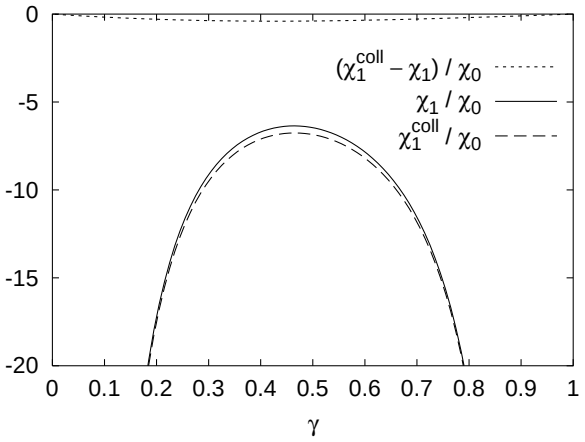

Fig. 9. A comparison of our collinear approximation and the full result for χ_1; $n_f = 0$.

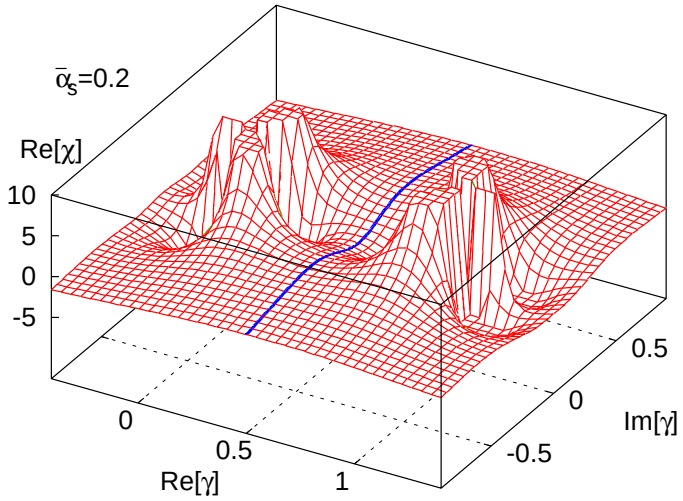

Fig. 10. The real part of the LL + NLL characteristic function for $\bar{\alpha}_s = 0.2$, together with the integration contour, in the complex plane.

3.5. Consequences of the NLL *corrections*

Figure 9 shows that the NLL corrections to χ are very large. For $\gamma = 1/2$ we have (again for $n_f = 0$)

$$\chi(1/2) = \chi_0(1/2)(1 - 6.47\bar{\alpha}_s)\,. \tag{55}$$

Thus for $\bar{\alpha}_{\rm s} = 0.2$, the predicted power is negative, at about -0.16, which is no more in agreement with the data than the leading power.

What is even more worrisome is that the structure of the characteristic function changes radically. In figure 6, there is a single saddle-point at $\gamma = 1/2$, *i.e.* on the real axis. With the NLL contributions included, there are now two saddle-points, at complex values of γ which we will call $\bar{\gamma}, \bar{\gamma}^*$ [10]. Since the cross section goes as

$$\sigma(s, Q^2, Q_0^2) \sim \left(\frac{s}{QQ_0}\right)^{\bar{\alpha}_{\rm s}\chi(\bar{\gamma})} \frac{1}{Q^2} \left(\frac{Q^2}{Q_0^2}\right)^{\bar{\gamma}} + \bar{\gamma} \leftrightarrow \bar{\gamma}^*, \tag{56}$$

the fact that $\bar{\gamma}$ is complex means that the cross section oscillates as a function of $\ln Q^2/Q_0^2$ (it remains real because of the contribution from the complex-conjugate saddle point). This behaviour occurs as long as χ has a negative second derivative at $\gamma = 1/2$, which is the case for $\bar{\alpha}_{\rm s} \gtrsim 0.05$. In other words there exists no phenomenologically accessible domain in which the inclusion of the NLL corrections gives a sensible result.

4. Beyond NLL

The solution is bound to lie with higher orders. Shortly after preliminary results on χ_1 had appeared, it was suggested that stable predictions might be obtained by inclusion of the NNLL and NNNLL terms [26]. But remembering that the LL calculation took about a year, and the NLL calculation ten years, a reasonable estimate for the time to calculate the NNLL terms might lie somewhere between an arithmetic (19 years) and a geometric (100 years) extrapolation. Even were these contributions to be calculated, there is actually no guarantee that the resulting series would converge for the values of $\bar{\alpha}_{\rm s}$ of interest!

So the only option left is to try and *guess* the higher-order terms and then to resum them (we are now talking about the resummation of a resummation). The question is whether there is some reliable way of guessing them. Various approaches have been investigated [12, 13, 27–29]. I here will advocate a method closely related to that used in the previous section to estimate the NLL corrections — namely a method based on the study of the collinear limit [12, 13].

We have already seen in the previous section that a study of the collinear limit is a powerful tool. For the NLL characteristic function it gave us the cubic and quadratic divergences at $\gamma = 0$ and $\gamma = 1$, and in the range $0 < \gamma < 1$ reproduced the full answer to remarkably good accuracy. How come?

There is a temptation to argue that since $\gamma = 1/2$ is a moderately small number, one can legitimately carry out an expansion in powers of γ and $1-\gamma$

(including the first two terms in the expansion for χ_0, *i.e.* the two poles and a constant, also seems to do quite well, reproducing the full answer to within about 8%). A slightly better motivated argument might be the following. For $\gamma = 1/2$, the transverse momentum integrals in the Mellin transform converge quite rapidly and so one might not expect a collinear approximation to work too well. However at higher orders, pieces of the transverse momentum integrals are accompanied by logarithms of transverse momentum. These have the effect of shifting the dominant part of the integral out towards more collinear regions, where the collinear approximation itself becomes better.

So there are reasons to believe that collinearly-enhanced contributions might give a significant part of the higher-order corrections even beyond NLL.[4] A more general justification for carrying out the collinear resummation is that one wants to be able to use one's answer in the collinear limit. Since the collinear limit involves taking γ close to zero, where higher orders involve successively more divergent terms, the only hope of a sensible answer there is a collinear resummation.

The determination of the collinearly enhanced corrections can be divided into two parts. The first deals with terms in the same class as the $1/\gamma^2$ terms in χ_1, single collinear logarithms originating from the splitting function and running coupling; the second addresses the terms in the same class as the $1/\gamma^3$ term in the NLL result, namely double collinear logarithms. We will consider only an outline of the method. The interested reader is referred to the original references [12, 13] for the full details.

4.1. Single collinear logs — running coupling and splitting function terms

It is fairly straightforward to calculate the collinear $\mathrm{N}^n\mathrm{LL}$ contributions to the BFKL kernel from splitting function and running coupling effects. One just takes diagrams such as figure 8 with an arbitrary number of non-small-x emissions, inserting and expanding the appropriate running coupling for each branching (the answer is given in [13]). One is then left with the tricky problem of resumming the resulting set of terms.

An equivalent approach essentially treats the small-x and non-small-x branchings on a more similar footing [13]. In eq. (28) we have a factor $\bar{\alpha}_{\mathrm{s}}/\omega$ coming from the $1/z$ part of the P_{gg} splitting function, and a factor of $\chi(\gamma)$ from the transverse structure of the branching. In the collinear limit, we can replace $1/\omega$ with the full splitting function, P^{ω}_{gg}. So the collinear behaviour

[4] This statement should really be restricted to those corrections that can be associated with a single ladder (referred to as t-channel iteration). Actually at NNLL, corrections arise associated with the presence of two ladders (the start of s-channel iteration), *i.e.* saturation, or unitarity corrections. Our aim here is to understand the high-energy behaviour of a single ladder.

of the $\bar{\alpha}_{\rm s}\chi/\omega$ factor becomes (for DIS energy scale, $s_0 = Q^2$)

$$\frac{\bar{\alpha}_{\rm s}P^{\omega}_{gg}}{\gamma} = \frac{\bar{\alpha}_{\rm s}(Q^2)}{\omega}\frac{1+\omega A_1(\omega)}{\gamma} \quad \Rightarrow \quad \chi \simeq \frac{1+\omega A_1(\omega)}{\gamma}\,, \tag{57}$$

where we have used eq. (38) for P^{ω}_{gg}. The correct scale in the branching is Q^2 (the largest scale in the problem) so there are no running coupling corrections.

The situation in the anti-collinear limit is very similar except for an issue related to the running coupling: the appropriate scale for the branching is not Q^2, but k^2 (referred to fig. 3). If we want to extract a factor of $\bar{\alpha}_{\rm s}(Q^2)$ the difference of scales must be taken into account. It turns out [13] that this can be done at all orders by replacing A_1 with $A_1 - b$, so that the resummed anti-collinear structure is (with the anti-DIS energy scale choice, $s_0 = Q_0^2$)

$$\frac{\bar{\alpha}_{\rm s}(Q^2)}{\omega}\frac{1+\omega(A_1(\omega)-b)}{1-\gamma} \quad \Rightarrow \quad \chi \simeq \frac{1+\omega(A_1(\omega)-b)}{1-\gamma}\,. \tag{58}$$

The reader can verify that substituting $\omega = \bar{\alpha}_{\rm s}\chi_0$ into the expressions for χ in (57) and (58) reproduces the correct NLL collinear-enhanced terms.

4.2. Double collinear logs — energy-scale terms

We have just given resummed answers for the collinear and anti-collinear behaviours of the kernel with DIS and anti-DIS energy scale choices respectively. We really want the answer for a common energy scale, say $s_0 = QQ_0$. We saw in section 3.3, that changes in s_0 introduce higher-order double-collinear logs (the $1/\gamma^3$ and $1/(1-\gamma)^3$ terms). The higher-order corrections had to be such that for energy scale $s_0 = Q^2$ there were no such terms around $\gamma = 0$, and similarly around $\gamma = 1$ for energy scale $s_0 = Q_0^2$. For $s_0 = QQ_0$, appropriate double-collinear log counterterms had to be included in order to satisfy the conditions for the other energy scales. One can work out, order by order, the counterterms for higher kernels, but it soon gets tedious. In any case one finds that the resulting series of terms is divergent for reasonable values of $\alpha_{\rm s}$.

The solution [12] exploits the fact that a change of energy scale corresponds to a shift of γ by an amount proportional to ω (*cf.* section 3.3). For energy scale $s_0 = QQ_0$, one writes a leading-order kernel with the following structure

$$\chi_0^{\omega} = 2\psi(1) - \psi\left(\gamma + \frac{\omega}{2}\right) - \psi\left(1 - \gamma + \frac{\omega}{2}\right), \qquad s_0 = QQ_0\,, \tag{59}$$

originally discussed in [30]. Changing energy scale to $s_0 = Q^2$ corresponds to the shift $\gamma \to \gamma - \frac{\omega}{2}$ (*cf.* section 3.3), and we have

$$\chi_0^\omega = 2\psi(1) - \psi\left(\gamma\right) - \psi\left(1-\gamma+\omega\right), \qquad s_0 = Q^2\,. \tag{60}$$

Remembering that $-\psi(\gamma) \simeq 1/\gamma$ for small γ, and iteratively solving for $\omega = \bar{\alpha}_{\rm s}\chi$ as we did in section 3.3, we find an answer which is free of singularities stronger than $1/\gamma$, and so free of spurious double collinear logs. The procedure can be repeated for energy scale $s_0 = Q_0^2$, expanding around $\gamma = 1$ and one finds an answer free of spurious double anti-collinear logs. Expanding (59) to order $\bar{\alpha}_{\rm s}$ gives exactly the same triple poles as in (51).

4.3. The full resummed answer

Let us first see how to correctly include the energy-scale resummation in the full kernel. We start with the modified LL characteristic function, χ_0^ω, eq. (59) which, as we have just seen, is free of unwanted double (anti) collinear logs for the (anti) DIS energy scale choice; χ_0^ω contains NLL corrections,

$$\frac{\chi_0}{2}\left(-\psi'(\gamma) - \psi'(1-\gamma)\right), \tag{61}$$

which must be subtracted from χ_1 to avoid double counting:

$$\tilde{\chi}_1 = \chi_1 - \frac{\chi_0}{2}\left(-\psi'(\gamma) - \psi'(1-\gamma)\right). \tag{62}$$

The quantity $\tilde{\chi}_1$ still has quadratic and single divergences at $\gamma = 0, 1$. In analogy with the single divergences in χ_0, these need to be 'shifted' in order to avoid spurious double-collinear logs at higher orders when changing energy scale. This is accomplished by subtracting unshifted divergences and replacing them with shifted divergences:

$$\begin{aligned}\tilde{\chi}_1^\omega = \tilde{\chi}_1 - A_1(0)\psi'(\gamma) + A_1(\omega)\psi'\left(\gamma+\frac{\omega}{2}\right) - (A_1(0)-b)\psi'(1-\gamma) \\ + (A_1(\omega)-b)\psi'\left(1-\gamma+\frac{\omega}{2}\right) + \frac{\pi^2}{6}\left(\chi_0^\omega - \chi_0\right).\end{aligned} \tag{63}$$

Here we have chosen to use $\psi'(\gamma)$ and $-\psi(\gamma)$ (in χ_0) as our quadratic and single 'divergences to be shifted'. We could equally well have used $1/\gamma^2$ and $1/\gamma$ respectively. The difference in the final result would amount to collinearly suppressed NNLL terms. The reason for including $A_1(\omega)$ in the shifted poles is discussed shortly.

To resum the splitting-function and running coupling effects, we have to ensure that χ has the following structure around $\gamma = 0$ and $\gamma = 1$,

$$\chi(\gamma,\omega) \simeq \frac{1+\omega A_1}{\gamma+\frac{\omega}{2}}, \qquad \gamma \ll 1\,, \tag{64a}$$

$$\chi(\gamma,\omega) \simeq \frac{1+\omega(A_1-b)}{1-\gamma+\frac{\omega}{2}}, \qquad 1-\gamma \ll 1\,, \tag{64b}$$

where the poles have been shifted compared to eqs. (57) and (58) to take into account that they have been written for energy scale $s_0 = QQ_0$. This can be obtained by writing

$$\chi(\gamma,\omega) = \chi_0^\omega + \omega\frac{\tilde{\chi}_1^\omega}{\chi_0^\omega}\,. \tag{65}$$

Since $\omega = \bar{\alpha}_{\rm s}\chi_0^\omega + \mathcal{O}\left(\bar{\alpha}_{\rm s}^2\right)$ the expansion of χ to order $\bar{\alpha}_{\rm s}$ is correct. Additionally the ratio $\tilde{\chi}_1^\omega/\chi_0^\omega$ contains (shifted) single poles at $\gamma = 0$ and $\gamma = 1$ with coefficients A_1 and $A_1 - b$ respectively, as required by eqs. (64). The full ω dependence of A_1 is included through the $A_1(\omega)$ factors eq. (63).

A point to note is that (65) is no longer an expansion in $\bar{\alpha}_{\rm s}$, but rather in ω. For this reason this resummation technique is known as the ω-expansion [13].

4.4. Results

Figure 11 shows various BFKL exponents as a function of $\bar{\alpha}_{\rm s}$, including the LL and NLL results for reference. The quantity labelled ω_s is the minimum value of $\omega = \bar{\alpha}_{\rm s}\chi(\gamma,\omega)$, and as such corresponds to the exponent expected for the gluon Green function at high energies. It is the power that one expects to observe in $\gamma^*\gamma^*$ collisions or forward-jet and Mueller-Navelet jet observables at *ep* and *pp* colliders respectively [22].

Also plotted is a second quantity labelled ω_c. This corresponds to the position of the singularity of the gluon anomalous dimension, *i.e.* the power growth of small-x splitting functions. Though we have not really discussed the resummed gluon anomalous dimension, it is worth noting that ω_c is significantly different from ω_s because it contains additional corrections $\mathcal{O}(\bar{\alpha}_{\rm s}^{5/3})$, which arise because the effective scale for BFKL evolution in the anomalous dimension turns out, dynamically, to be considerably higher than Q^2. Corrections of this form were first noticed in [31]. In general, such corrections are present for quantities involving an effective cutoff on the lowest accessible transverse momentum. Another example of such a quantity is the elastic-scattering cross section. It should be emphasised therefore that the

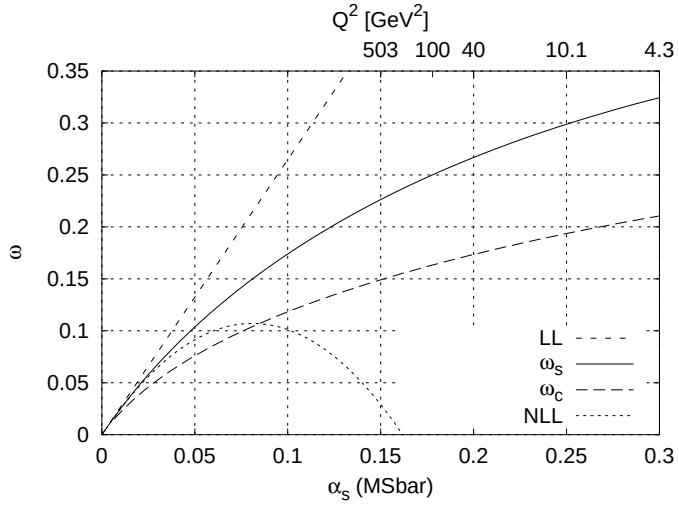

Fig. 11. Various BFKL exponents

difference between ω_s and ω_c is not an uncertainty on the BFKL exponent, but rather reflects differences between various processes.

The actual uncertainty on the results can be determined by examining the effect of scheme changes and different approaches to the details of the resummation (as discussed for example in the previous section, with regards to the shifting of divergences), as well as a study of solvable models [22] or other possible higher-order effects [29]. For $\bar{\alpha}_{\rm s} \simeq 0.2$ it is about 15%.

5. Conclusions and Outlook

In these lectures, we have seen how to deduce many of the properties of the BFKL pomeron. The recurrent theme has been the study of the collinear (and anti-collinear) limit, which gives information about the structure of divergences of the BFKL characteristic function at all orders. At NLL order the information thus obtained is sufficient to reproduce the true NLL corrections to a high degree of accuracy, *i.e.* the non-collinearly enhanced NLL corrections are small. Ensuring that the BFKL kernel correctly reproduces the collinear limit at all orders leads to stable predictions for the high-energy power growth. The resulting resummed power is much more compatible with the data than either the LL or NLL values.

For actual phenomenology, two more ingredients are required. First we should understand the exponentiation of the characteristic function, because the running of the coupling complicates the simple approach that we had at leading order — it turns out however that these complications are not too

severe [11, 22, 32].

Secondly we need to know the virtual photon impact factors, *i.e.* the coupling of a virtual photon (DIS or $\gamma^*\gamma^*$) to the gluon chain. These have still to be worked out at NLL. When results are eventually available it is likely that a collinear resummation will again be needed in order to obtain stable predictions, in analogy with the situation for the characteristic function.

The overall message is that despite initial fears, the large size of the NLL corrections BFKL is not an impediment to the use of BFKL resummation for predicting high-energy phenomena. But it is necessary to understand the origin of the large corrections, and include at all orders the physics which causes them.

Acknowledgements

Some of the results presented here were obtained in collaboration with Marcello Ciafaloni and Dimitri Colferai. In writing these lectures I have benefited also from conversations with Martin Beneke, Carlo Ewerz and Maneesh Wadhwa. Finally I would like to thank the organisers of the School for the welcoming and stimulating environment that they provided.

REFERENCES

[1] L.N. Lipatov, *Sov. J. Nucl. Phys.* **23** (1976) 338;
E.A. Kuraev, L.N. Lipatov and V.S. Fadin, *Sov. Phys.* JETP **44** (1976) 443;
E.A. Kuraev, L.N. Lipatov and V.S. Fadin, *Sov. Phys.* JETP **45** (1977) 199;
Ya. Balitskii and L.N. Lipatov, *Sov. J. Nucl. Phys.* **28** (1978) 822.

[2] H1 Collaboration (Adloff et al.), *Nucl. Phys.* **B 470** (1996) 3 [hep-ex/9603004].

[3] ZEUS Collaboration (Breitweg et al.), *Phys. Lett.* **B 407** (1997) 402 [hep-ex/9706009].

[4] L3 Collaboration (M. Acciarri et al.), *Phys. Lett.* **B 453** (1999) 333.

[5] OPAL collaboration, physics note 391, contribution to Lepton-Photon '99, Stanford, August 1999.

[6] ZEUS Collaboration (J. Breitweg et al.), *Eur. Phys. J.* **C6** (1999) 239;
H1 Collaboration (C. Adloff et al.), *Nucl. Phys.* **B 538** (1999) 3.

[7] L.N. Lipatov and V.S. Fadin, *Sov. J. Nucl. Phys.* **50** (1989) 712;
V.S. Fadin, R. Fiore and M.I. Kotsky, *Phys. Lett.* **B 359** (1995) 181;
V.S. Fadin, R. Fiore and M.I. Kotsky, *Phys. Lett.* **B 387** (1996) 593 [hep-ph/9605357];
V.S. Fadin, and L.N. Lipatov, *Nucl. Phys.* **B 406** (1993) 259;
V.S. Fadin, R. Fiore and A. Quartarolo, *Phys. Rev.* **D 50** (1994) 5893 [hep-th/9405127];

V.S. Fadin, R. Fiore, and M. I. Kotsky, *Phys. Lett.* **B 389** (1996) 737 [hep-ph/9608229];
V.S. Fadin and L.N. Lipatov, *Nucl. Phys.* **B 477** (1996) 767 [hep-ph/9602287];
V.S. Fadin, M.I. Kotsky and L.N. Lipatov, *Phys. Lett.* **B 415** (1997) 97;
S. Catani, M. Ciafaloni and F.Hautman, *Phys. Lett.* **B 242** (1990) 97;
S. Catani, M. Ciafaloni and F.Hautman, *Nucl. Phys.* **B 366** (1991) 135;
V. S. Fadin, R. Fiore, A. Flachi, and M. I. Kotsky, *Phys. Lett.* **B 422** (1998) 287 [hep-ph/9711427];
V. Del Duca, *Phys. Rev.* **D 54** (1996) 989;
V. Del Duca, *Phys. Rev.* **D 54** (1996) 4474;
V. Del Duca and C.R. Schmidt, *Phys. Rev.* **D 57** (1998) 4069 [hep-ph/9711309];
V. Del Duca and C.R. Schmidt, *Phys. Rev.* **D 59** (1999) 074004 [hep-ph/9810215].

[8] V.S. Fadin and L.N. Lipatov, *Phys. Lett.* **B 429** (1998) 127 [hep-ph/9802290].

[9] M. Ciafaloni and G. Camici, *Phys. Lett.* **B 412** (1997) 396 [hep-ph/9707390];
M. Ciafaloni, *Phys. Lett.* **B 429** (1998) 363 [hep-ph/9801322];
M. Ciafaloni and G. Camici, *Phys. Lett.* **B 430** (1998) 349 [hep-ph/9803389].

[10] D.A. Ross, *Phys. Lett.* **B 431** (1998) 161 [hep-ph/9804332].

[11] E. Levin, hep-ph/9806228.

[12] G.P. Salam, JHEP **9807** (1998) 19 [hep-ph/9806482].

[13] M. Ciafaloni and D. Colferai, *Phys. Lett.* **B 452** (1999) 372 [hep-ph/9812366];
M. Ciafaloni, D. Colferai and G.P. Salam, hep-ph/9905566.

[14] V.N. Gribov and L.N. Lipatov, *Sov. J. Nucl. Phys.* **15** (1972) 438;
G. Altarelli and G. Parisi, *Nucl. Phys.* **B 126** (1977) 298;
Yu.L. Dokshitzer, *Sov. Phys.* JETP **46** (1977) 641.

[15] M. Abramowitz and I. Stegun, *Handbook of Mathematical Functions*, Dover Publications.

[16] A. De Rujula, S.L. Glashow, H.D. Politzer, S.B. Treiman, F. Wilczek and A. Zee, *Phys. Rev.* **D 10** (1974) 1649.

[17] M. Gluck, E. Reya and A. Vogt, *Z. Physik* **C 67** (1995) 433.

[18] R.D. Ball and S. Forte, *Phys. Lett.* **B 335** (1994) 77 [hep-ph/9405320].

[19] A.H. Mueller, *Nucl. Phys.* **B 415** (1994) 373;
A.H. Mueller and B. Patel, *Nucl. Phys.* **B 425** (1994) 471 [hep-ph/9403256;
N.N. Nikolaev and B.G. Zakharov, JETP *Lett.* **59** (1994) 6 [hep-ph/9312268];
see also the introduction to the dipole approach in R.K. Ellis, W.J. Strling and B.R. Webber, *QCD and Collider Physics*, Cambridge University Press, 1996.

[20] J.R. Forshaw and D.A. Ross, *Quantum Chromodynamics and the Pomeron*, Cambridge University Press, 1997.

[21] J. Kwiecinski, *Z. Physik* **C 29** (1985) 561;
J.C. Collins and J. Kwiecinski, *Nucl. Phys.* **B 316** (1989) 307.

[22] M. Ciafaloni, D. Colferai and G.P. Salam, JHEP **10** (1999) 017 [hep-ph/9907409].

[23] R.D. Ball and S. Forte, *Proceedings of the DIS 96 Workshop*, 1996, p. 208 [hep-ph/9706291].

[24] P. Achard (for the L3 collaboration), talk given at Photon 99, Freiburg, Germany, hep-ex/9907016;
Maneesh Wadhwa, talk given at 19th International Conference on Physics in Collision (PIC 99), Ann Arbor, MI, hep-ex/9909001.

[25] S. Catani, G. Marchesini and B.R. Webber, *Nucl. Phys.* **B 349** (1991) 635;
Yu.L. Dokshitzer, V.A. Khoze and S.I. Troyan, *Phys. Rev.* **53** (1996) 89.

[26] J. Blümlein and A. Vogt, *Phys. Rev.* **D 57** (1998) 1 [hep-ph/9707488];
J. Blümlein and A. Vogt, *Phys. Rev.* **D 58** (1998) 014020 [hep-ph/9712546].

[27] C. Schmidt, *Phys. Rev.* **D 60** (1999) 074003 [hep-ph/9901397].

[28] S.J. Brodsky, V.S. Fadin, V.T. Kim, L.N. Lipatov and G.B. Pivovarov, JETP *Lett.* **70** (1999) 155 [hep-ph/9901229].

[29] J.R. Forshaw, D.A. Ross and A. Sabio Vera, *Phys. Lett.* **B 455** (1999) 273 [hep-ph/9903390].

[30] B. Andersson, G. Gustafson and J. Samuelsson, *Nucl. Phys.* **B 467** (1996) 443.

[31] R.E. Hancock and D.A. Ross, *Nucl. Phys.* **B 383** (1992) 575;
R.E. Hancock and D.A. Ross, *Nucl. Phys.* **B 394** (1993) 200;
see also [20].

[32] Yu.V. Kovchegov and A.H. Mueller, *Phys. Lett.* **B 439** (1998) 428 [hep-ph/9805208].